IEEE Access
Multidisciplinary | Rapid Review | Open Access Journal

Received August 26, 2021, accepted September 10, 2021, date of publication September 17, 2021,
date of current version September 27, 2021.

Digital Object Identifier 10.1109/ACCESS.2021.3113767

Toward a More Realistic Characterization of Hand-Assembled Wire Bundles: Geometrical Modeling and EMC Prediction

XIAOKANG LIU, (Member, IEEE), FLAVIA GRASSI, (Senior Member, IEEE), GIORDANO SPADACINI, (Senior Member, IEEE), AND SERGIO AMEDEO PIGNARI, (Fellow, IEEE)
Dipartimento di Elettronica Informazione e Bioingegneria, Politecnico di Milano, 20133 Milan, Italy
Corresponding author: Xiaokang Liu (xiaokang.liu@polimi.it)

ABSTRACT In this paper, a systematic approach for electromagnetic compatibility (EMC) modelling of hand-assembled, complex cable bundles is presented. The first part of the article focuses on bundles laid out above a ground plane, with layout approximately parallel to the reference ground. In order to generate smooth and physics-based trajectories, polynomial curves are used to represent the conductors in the bundle. A suitable process for the generation of bundle samples is developed, which allows for controlling the degree of randomness and avoiding conductors overlapping. Parametric representation of more general bundle structures with arbitrary orientation is then addressed, and the modeling approach is extended to more complex bundle structures, such as bundles involving twisted-wire pairs. To assess the ability of Transmission Line (TL) theory to deal with complex and locally highly non-uniform bundle shapes, a fictitious bundle trajectory shaped as a trefoil knot is introduced. All the generated bundle geometries are used in combination with TL-based EMC models in order to predict the disturbances induced in the bundle terminal units due to crosstalk or coupling with external electromagnetic fields. Prediction accuracy is assessed by comparison versus full-wave electromagnetic simulation of the same bundle structures. Suitable examples are presented to show the high numerical efficiency and good accuracy of the proposed modeling approach, as well as the need for accurate and physics-based representation of the bundle geometry in order to achieve solid EMC prediction in a wide frequency range.

INDEX TERMS Crosstalk, field-to-wire coupling, physically based modeling, random wire bundles, nonuniform transmission lines.

I. INTRODUCTION

Accurate prediction of electromagnetic compatibility (EMC) performance of hand-assembled wire bundles is a challenge for EMC engineers. Indeed, in several industrial sectors, [1]–[5], harnesses with length up to several hundred meters and exhibiting random wire arrangement are often employed (e.g., in the Electrical Wiring Interconnection Systems of aircrafts). These geometrical characteristics make difficult the development of prediction models effective both in terms of accuracy and of computational times, as well as the design of proper mitigation techniques ensuring system reliability. In this framework, further investigations are still required to provide an accurate description of the bundle geometry and to develop computationally-effective prediction of the involved electromagnetic (EM) phenomena, which are crucial steps to provide essential information about the amount of noise induced at the bundle terminal loads.

From the perspective of geometrical modelling, several methods have been proposed in recent years under the simplifying assumption that the bundle axis runs approximately parallel to ground [1], [6]–[11]. These models provide a roughly-discretized representation of the bundle geometry, suitable for subsequent numerical solution of the pertinent transmission-line (TL) equations, but often leading to violations of basic physical constraints, such as wire *continuity* and *non-overlapping* [12]. Among these, the *random midpoint displacement* algorithm [6], [7], was proposed to describe

The associate editor coordinating the review of this manuscript and approving it for publication was Wen-Sheng Zhao.

randomness of the wire trajectories by subdividing the bundle into uniform cascaded segments and representing the wire positions by fractal curves. This method controls wire continuity within the bundle, yet the adopted anti-overlapping algorithm may lead to discontinuities between adjacent segments. Later, the *random displacement spline interpolation* algorithm was adopted in [8] to reduce wire discontinuity along the bundle length and speed-up the computation of the per-unit-length parameters. This approach provides a better representation of the wire paths, but the transitions between adjacent segments still involve discontinuities as large as the wire diameter due to re-mapping of the actual wire positions into pre-defined reference cross-sections along the bundle axis. In [9], the random generation of bundle structure is done with a pseudo-random algorithm, which incorporates the constraints of proximity and non-overlapping at discrete cross-sections. However, non-smooth and overlapping trajectories can be observed along the bundle. The approach proposed in [1] exploits Graph Theory to assure minimum-distance wire movements across adjacent bundle segments, meanwhile effectively avoiding wire overlapping. However, in spite of its computational effectiveness (of paramount importance in view of statistical analysis), this algorithm also leads to discontinuities in wire trajectory as large as one wire diameter, since wires can just swap their positions over a reference cross-section, which is invariant all along the bundle. To avoid discontinuities owing to abrupt changes in wire positions (often leading to spurious resonances in the frequency response of voltages and currents at the bundle terminals), the approach in [12] proposes the use of a polynomial-based parameteric representation of wire trajectories in combination with a suitable anti-overlapping algorithm.

This article retains the parametric polynomial-based representation of wire trajectories in [12] as the starting point to develop a more general and comprehensive modeling framework aimed at modelling the complexity and randomness of actual bundle geometries. As the first step, the modeling procedure in [12] is reformulated to (a) account for bundle variation in the three dimensions, and (b) represent more complex wiring structures, e.g., bundles of twisted-wire pairs (TWPs). Then, in order to overcome the limitation that, in spite of the aforesaid reformulation, the procedure inherently allows to model bundles approximately stretched along the longitudinal axis with limited variation in the orthogonal directions (i.e., bundle parallel or nearly-parallel to ground), a 3-D rotational frame (i.e., the Frenet frame) is introduced to extend the analysis to arbitrarily-oriented wiring structures. Also, practical rules are provided to effectively interconnect different bundle models generated by the proposed algorithms, so to obtain complex and arbitrarily-oriented bundle geometries without violation of physical constraints in terms of *continuity*, *smoothness*, and *not-overlapping* of wire trajectories as well as *compactness* of the cable cross-section.

The obtained parametric representation of the bundle geometry can be easily imported into commercial EM solvers for prediction of EMC performance (e.g., prediction of voltages/currents induced by near-field or far-field coupling). In the work, full-wave simulations based on the method of moments (MoM) simulations are used as reference for investigating the accuracy of prediction models based on TL theory, which for highly-nonuniform structures, as those here considered, can provide an approximate yet more computationally-efficient prediction of induced voltages/currents. In this regard, previous studies, e.g., [12], have already proved the feasibility and accuracy of TL-based solution approaches for bundle structures running nearly parallel to ground in spite of line non-uniformity. However, for more complex geometries, the strong non-uniformity with respect to ground may compromise the basic assumptions of TL theory, with consequent degradation of TL prediction accuracy. To address this issue, the article introduces a 7-wire and a 7-TWP bundles with a knot in the middle, obtained by interconnecting three bundle sections generated by the proposed algorithms, as test cases. Crosstalk and radiated susceptibility performance of these harnesses are investigated by full-wave and TL-based simulation, by predicting the voltages induced at the terminations of the wires in the bundles up to 2 GHz.

The article is organized as follows. In Sec. II, geometrical modelling of different bundle structures are introduced, along with practical rules to interconnect different bundle segments. Sec. III explains how the generated bundle geometries can be effectively used in combination with full-wave and TL-based simulation in order to predict EMC performance. In Sec. IV, examples of crosstalk and radiated susceptibility predictions are presented, involving a 7-wire and a 7-TWP bundle with a knot in the middle as test cases. Conclusions are eventually drawn in Sec. V.

II. GEOMETRICAL BUNDLE REPRESENTATION

A. BUNDLES APPROXIMATELY PARALLEL TO GROUND

1) PHYSICAL CONSTRAINTS AND MODELING FRAMEWORK

The modelling technique in [12] foresees to represent wire paths inside the bundle through piece-wise or global polynomial expressions of their trajectories along the longitudinal bundle axis. Since piece-wise polynomial representation requires wire separation in the order of 6 times the wire radius (*loose bundle* condition in [12], Fig. 3), the representation with global polynomial expressions is here preferred. Namely, with reference to the Euclidean coordinate system in Fig. 1, each wire i inside a N-wire bundle is modelled by the trajectory of its center point, (x_i, y_i, z), where x_i and y_i are analytical functions of z (the longitudinal axis). Without loss of generality, here all wires inside the bundle have the same radius, r, and total axial length L. Besides, the bundle is characterized by an external circular contour with radius r_0 and a variable average height along the longitudinal axis, $h(z)$.

Each wire trajectory needs to obey the mathematical constraints in Tab. 1, which differ from those in [12] since here possible variations in the 2 directions are allowed. These constraints are aimed at assuring wire continuity as well as cross-section compactness along the bundle axis yet avoiding wire overlapping.

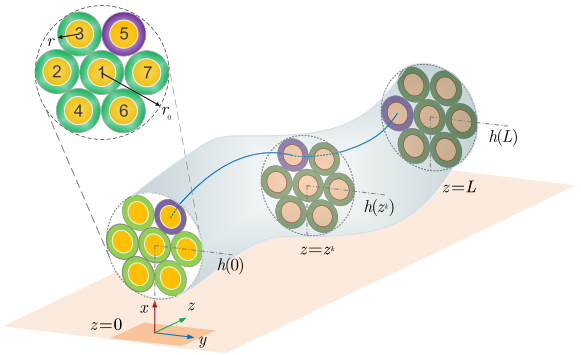

FIGURE 1. Reference coordinate frame for bundles approximately parallel to ground.

TABLE 1. Physical constraints for a random wire bundle approximately parallel to ground.

Constraint	Mathematical Representation
Non-overlapping	$2r \le \sqrt{[x_i(z)-x_j(z)]^2+[y_i(z)-y_j(z)]^2}$, $i,j=1,\ldots,N; i<j$
Continuity	$\lim_{z_i\to z^{k+}} x_i(z_i) = \lim_{z_i\to z^{k-}} x_i(z_i) = x_i(z_i)$, $\lim_{z_i\to z^{k+}} y_i(z_i) = \lim_{z_i\to z^{k-}} y_i(z_i) = y_i(z_i)$, $i=1,\ldots,N, z^k\in(0,L)$
Compactness	$\sqrt{[x_i(z)-h(z)]^2+y_i^2(z)}+r\le r_0$, $i=1,\ldots,N$

Under such preliminary assumptions, the wire bundle can be fully described by $2N$ sets of analytical functions (i.e., N for x- and N for y-axis characterization). In compact form, they write

$$\mathbf{x}(z)=\mathbf{C}^{(x)}\mathbf{b}(z);\quad \mathbf{y}(z)=\mathbf{C}^{(y)}\mathbf{b}(z) \tag{1}$$

where $\mathbf{x}(z)$, $\mathbf{y}(z)$ are $N\times 1$ function vectors, representing the vertical and horizontal direction coordinates of each wire along the z-axis; $\mathbf{b}(z)$ is a $M\times 1$ vector of basis functions, with $M-1$ the highest order of the exploited function; $\mathbf{C}^{(x,y)}$ are $N\times M$ matrices whose entries are to be determined by the bundle generation algorithm.

The basis functions in (1) are preliminarily determined by numerical computational methods, so to assure wire smoothness. To identify the best set of basis functions, two possible sets, i.e. the polynomial- and Fourier-type functions (see Tab. 2) are investigated by using the same ordinary least-square method for coefficients fitting. The obtained results showed that use of polynomial basis functions leads to an improvement of 2–3× times in generation efficiency w.r.t. Fourier-type ones, for bundles with low/medium complexity (length from 0.5–5 m, and number of conductors from 7 to 19). Hence, the polynomial basis functions are selected, and a suitable order, M, is chosen so to represent all curving features yet avoiding singular coefficient matrices in the least-square fit calculation. The entries of matrices $\mathbf{C}^{(x)}$, $\mathbf{C}^{(y)}$ are then evaluated by means of an iterative process [12], by making use of: (a) the mature algorithm based on Graph Theory [1] for the generation of intermediate reference cross-sections through the concept of *cycle* (used to describe wire movements between two adjacent cross-sections), (b) a suitable polynomial interpolation algorithm and (c) an *ad-hoc* algorithm for detecting and eliminating possible wire overlapping. A final check ensures the bundle properly fits into polynomial functions, and the analytical representation of the bundle satisfies the geometrical constraints in Tab. 1.

TABLE 2. Basis function sets for proposed bundle generation algorithm.

Func. set	Subset	Basis function
Polynomial	–	$[1, z, z^2, \ldots, z^{M-1}]^t$
Fourier	all terms	$[1, \cos(t), \cos(2t), \ldots, \cos[(M-1)t], \sin(t), \sin(2t), \ldots, \sin[(M-1)t]]$
	cos-only	$[1, \cos(t), \cos(2t), \ldots, \cos[(M-1)t]]$
	sin-only	$[1, \sin(t), \sin(2t), \ldots, \sin[(M-1)t]]$

2) MODELING GEOMETRICAL VARIATION IN 3-DIMENSIONS

In previous works (e.g., [1], [8]), bundles with constant height above ground and no horizontal (y-axis direction) variation are commonly assumed. This assumption is in line with practical setups for EMC testing, where bundles with a nominal, constant height above ground are often suggested. Also, it allows for significant simplification of the EMC prediction model. Nevertheless, in practical installations and experimental setups, the bundle structure can be slightly (e.g., as illustrated in Fig. 1) or severely curved.

From the viewpoint of modelling, these geometrical variations will be modelled as axial movement of the bundle axis superimposed to longitudinal variations of the rate of rotation around the cable axis, as it will be explained in the following paragraph. For simplicity, all transverse cross-sections of the bundle will be assumed to retain circular shape (assumption which is valid as long as variations are limited). Moreover, the *compactness* constraint in [12] will be modified to allow for a place-dependent height above ground, $h(z)$ (see Tab. 1).

(1) Modeling Axial Movements: Axial movements of the bundle in the x- and y- directions are readily implemented by introducing variations in the position of intermediate cross-sections. For instance, to model a variable bundle height w.r.t. the longitudinal position, at the beginning of the generation procedure, a variation $\Delta h(z^k)$ is added to the x-coordinate of the centers of all wires belonging to the reference cross-section z^k (see [12], Sec. III-A). In case of high curvature levels, this may require to properly increase the order of basis functions to retain the complexity of the original curve.

To better reflect the randomness of the bundle geometry, random variations in each dimension can be modeled by a continuous-space stochastic process (SP). For example, considering the bundle height along longitudinal axis, it can be modelled as a Gaussian SP as:

$$h(z)\sim\mathcal{N}(h_{\text{nom}},\sigma) \tag{2}$$

where $\mathcal{N}$ is the normal distribution; h_{nom} and σ are the mean value (i.e. average height) and standard deviation. Additionally, the covariance of $h(z)$ satisfies [13]

$$\begin{aligned}\text{cov}[h(z_1),h(z_2)] &= E[h(z_1)h(z_2)]-h_{\text{nom}}^2\\ &= c(|z_2-z_1|)\end{aligned} \tag{3}$$

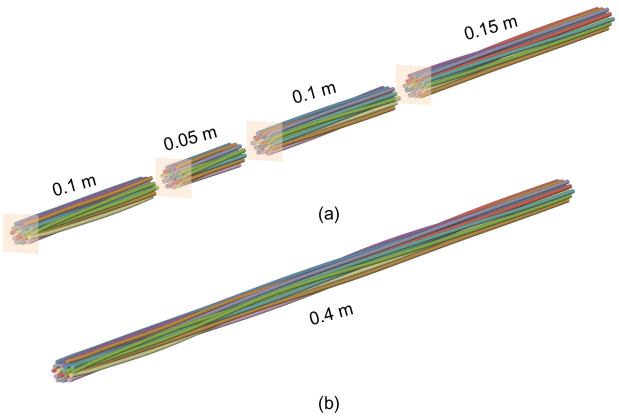

FIGURE 2. Example of a wire bundle with variable section lengths. (a) Generated sections with different lengths, and (b) whole structure.

where $E(\cdot)$ and $\mathrm{cov}(\cdot,\cdot)$ denote the expectation and covariance operators, respectively. In accordance with the assumption in [13], an efficient covariance function can be defined as

$$c(\tau) = \sigma^2 e^{-\frac{\tau^2}{\rho^2}} \tag{4}$$

where ρ is the covariance range determining the rapidity of the variation of $h(z)$.

(2) Modeling Variations in the Longitudinal Rate of Rotation: Variations in the longitudinal rate of rotation of wires around the cable axis is strictly related to the frequency by which wires exchange their position along the cable axis. This parameter is actually determined by several factors, including the level of twisting, the number of wires, the separation between wires (if wires are loosely or tightly bundled), the possible presence of lacing cords and so on. For hand-assembled bundles, it can be estimated (as an average parameter) by bundle inspection, e.g., subdividing a 1-m bundle into 10 uniform sections seems a good choice for slightly-twisted bundles composed of 7 wires [12]. In the proposed algorithm this parameter can be easily set, by suitably selecting the number and distribution of intermediate cross-sections along the bundle so to readily increase/decrease and/or make the rotation rate non-uniform along the bundle length. As an example, in Fig. 2, a dense bundle with $N = 19$ wires and variable section length generated by the proposed algorithm is shown. The bundle longitudinal length L is 0.4 m with 4 sections. The wire radius $r = 0.5$ mm and the wire separation, s, is $s = 2.5r$.

3) MODELING BUNDLE OF TWPs

The proposed approach can be easily extended to the generation of bundles composed of TWPs, by interpreting the trajectory of each wire inside the original bundle as the trajectory of the corresponding TWP axis.

By making use of the notation in Fig. 3, the place-dependent coordinates of wire A and B in the i-th TWP read

$$\begin{aligned} x_{\substack{A\\B}}^{\mathrm{TWP},i}(z) &= x_i(z) \pm \frac{d_i}{2}\sin(\varphi_i(z)) \\ y_{\substack{A\\B}}^{\mathrm{TWP},i}(z) &= y_i(z) \pm \frac{d_i}{2}\cos(\varphi_i(z)) \end{aligned} \tag{5}$$

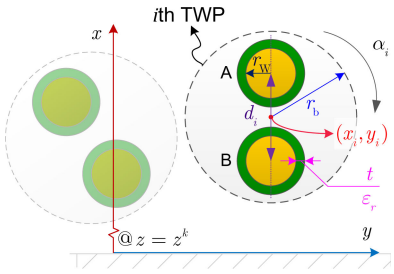

FIGURE 3. Cross-section view of TWP inside bundle.

where d_i denotes wire separation ($0 < d_i < 2r_b$), and φ_i the place-dependent rotational angle. If a constant twist-pitch, p_i, is considered, φ_i takes the expression

$$\varphi_i(z) = \alpha_i + 2\pi p_i z \tag{6}$$

where $\alpha_i \in [0, 2\pi]$ is the initial twisting angle at $z = 0$.

As an illustrative example, Fig. 4 shows a random bundle of 19 TWPs generated by the proposed algorithm. Variations in the x- and y-directions are also included.

B. ARBITRARILY SHAPED BUNDLE STRUCTURES

1) PARAMETRIC REPRESENTATION OF WIRE TRAJECTORIES

To describe arbitrarily-oriented bundle structures, with axis no longer parallel or nearly-parallel to ground as in the previous cases, a reference trajectory is introduced, and modeled by a parametric curve in the 3-D Euclidean space. With reference to the right-handed orthonormal system in Fig. 5, the reference trajectory is expressed as function of the independent variable u, $u \in [U_{\mathrm{lower}}, U_{\mathrm{upper}}]$, by the curve $\mathbf{Q}(u) = [x(u), y(u), z(u)]$, where $x(u)$, $y(u)$ and $z(u)$ denote the vertical, horizontal, and longitudinal coordinate functions, respectively.

Wire bundles approximately parallel to the ground (Sec. II-A) represent a special case, requiring a stationary instead of a rotational reference frame, which can be obtained by enforcing $z_i(u) = u$ $(i = 1, 2, \ldots, N)$ as longitudinal-axis coordinate functions.

2) ROTATIONAL FRAME AND BUNDLE REPRESENTATION

To model a bundle of wires starting from the reference path, $\mathbf{Q}(u)$, the Frenet frame is here exploited, which represents a smoothly varying coordinate system along a 3D curve, characterized by three orthogonal axis vectors [14], i.e.,

- a normalized tangent vector, $\mathbf{t}(u)$,

$$\mathbf{t}(u) = \frac{\mathbf{Q}'(u)}{\|\mathbf{Q}'(u)\|} \tag{7}$$

- a normalized binormal vector, $\mathbf{b}(u)$,

$$\mathbf{b}(u) = \frac{\mathbf{Q}'(u) \times \mathbf{Q}''(u)}{\|\mathbf{Q}'(u) \times \mathbf{Q}''(u)\|} \tag{8}$$

- a normalized normal vector, $\mathbf{n}(u)$,

$$\mathbf{n}(u) = \frac{\mathbf{b}(u) \times \mathbf{t}(u)}{\|\mathbf{b}(u) \times \mathbf{t}(u)\|} \tag{9}$$

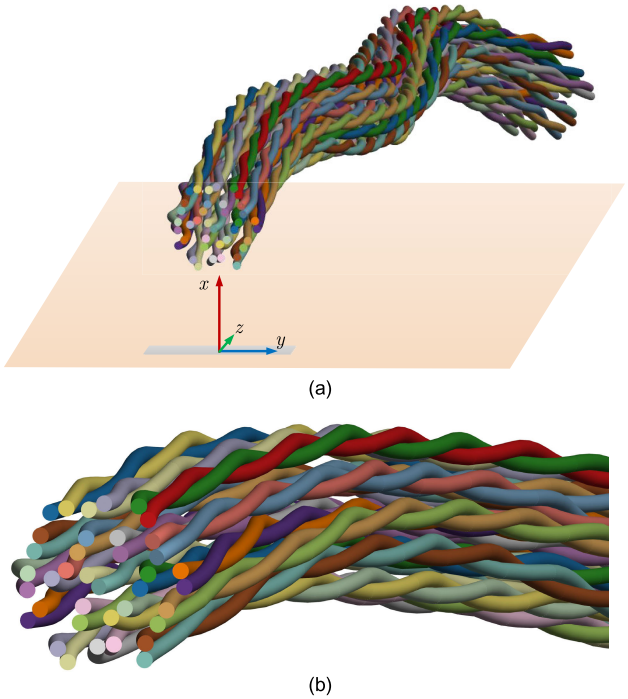

FIGURE 4. Generated bundle of 0.5-m longitudinal length and 19 TWPs with horizontal/vertical variation: (a) overall view; (b) a zoom-in at the terminal end.

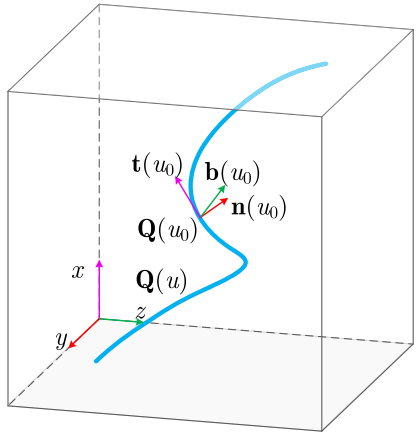

FIGURE 5. 3-D wire trajectory $\mathbf{Q}(u)$ in the Euclidean frame, and Frenet frame vectors at $\mathbf{Q}(u_0)$.

Based on the above base of normalized vectors, a wire i inside the bundle is represented by its trajectory as the combination of the reference trajectory $\mathbf{Q}(u)$ and its pertinent offset in the orthonormal plane as

$$\mathbf{Q}_i(u) = \mathbf{Q}(u) + \kappa_{1,i}(u)\mathbf{n}(u) + \kappa_{2,i}(u)\mathbf{b}(u) \tag{10}$$

According to this formalism, a bundle composed of N parallel wires is modelled by invariant $\kappa_{1,i}(u)$ and $\kappa_{2,i}(u)$ functions. Conversely, to model more complex wire arrangements (e.g., a wire/TWP-bundle with randomized wire allocation), the contour-related functions $\kappa_{1,i}(u)$ and $\kappa_{2,i}(u)$ are locally modified while imposing the constraints of wire *continuity* and *non-overlapping* along the bundle path $\mathbf{Q}(u)$.

For instance, the pair of twisted wires inside a TWP bundle introduced in Sec. II-A3 is modelled as

$$\mathbf{r}_{\substack{A\\B}}^{\mathrm{TWP},i}(u) = \mathbf{Q}(u) + \left[\kappa_{1,i}(u) \pm \frac{d_i}{2}\sin(\varphi_i(u))\right]\mathbf{n}(u) + \left[\kappa_{2,i}(u) \pm \frac{d_i}{2}\cos(\varphi_i(u))\right]\mathbf{b}(u) \tag{11}$$

where $\varphi_i(u)$ denotes the pertinent rotational angle function w.r.t. variable u. For arbitrarily-oriented bundles, such a function, i.e.,

$$\varphi_i(u) = \alpha_i + 2\pi p_i \ell_i(u) \tag{12}$$

may be no longer linear, since it is strictly dependent on the wire curvilinear abscissa $\ell_i(u)$, i.e.,

$$\ell_i(u) = \int_{u_{\mathrm{lo},i}}^{u} \left\|\mathbf{Q}'_i(u)\right\| du \tag{13}$$

where $u_{\mathrm{lo},i}$ denotes the lower limit of the i-th TWP trajectory.

In general, solution of the integral in (13) requires numerical integration. However, if an analytical expression of $\ell_i(u)$ is required (for instance, if the geometry needs to be imported into an EM solver), this can be obtained afterwards by adopting curve-fitting (e.g. polynomial fitting) techniques.

C. INTERCONNECTION OF BUNDLE STRUCTURES

In order to reproduce the complexity of actual wiring harnesses, there is often the need to combine and interconnect different cable sections. To this end, this subsection will introduce practical rules to connect different bundle segments obtained by the proposed generation algorithms. This goal is achieved by combining the polynomial function representation in Sec. II-A with proper constraints, assuring *continuity* as well as *smoothness* (enforced in terms of continuity of the first order derivatives) of wire trajectories. To this end, suitable linear equality constraints are enforced when solving the least-squares problem during the curve fitting process. For the connection of TWP bundles (not considered here for the sake of brevity), additional attention should be paid in determining the initial twisting angles of each bundle segment, so to assure a smooth wire transition.

1) CONNECTING BUNDLES APPROXIMATELY PARALLEL TO GROUND

In general, direct connection of two bundles generated by the proposed algorithm (Sec. II-A) may lead to a violation of the constraint of wire *continuity*. As a matter of fact, to avoid overlapping, the generation algorithm unpredictably perturbs the arrangement of wires with respect to their original position in the reference cross-section, as shown in the left panel of Fig. 6. Hence, additional constraints are included in the generation process of both bundles, to control wire position at the interface section, thus assuring wire continuity. For two bundles denoted as #1 and #2, these constraints are

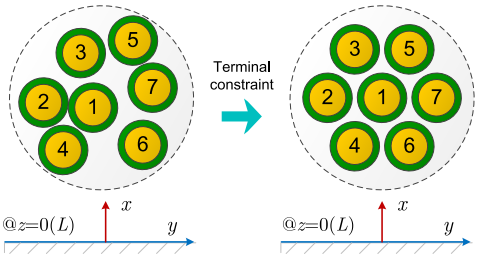

FIGURE 6. Examples of terminal cross-sections obtained without (left) and with (right) enforcing the additional terminal constraints in (14).

formulated as

$$\begin{cases} \mathbf{x}_{\#1}(z) = \mathbf{C}_{\#1}{}^{(x)}\mathbf{b}_{\#1}(z) \\ \mathbf{y}_{\#1}(z) = \mathbf{C}_{\#1}{}^{(y)}\mathbf{b}_{\#1}(z) \\ \mathbf{x}_{\#2}(z) = \mathbf{C}_{\#2}{}^{(x)}\mathbf{b}_{\#2}(z) \\ \mathbf{y}_{\#2}(z) = \mathbf{C}_{\#2}{}^{(y)}\mathbf{b}_{\#2}(z), \end{cases}$$
$$s.t. \begin{cases} \mathbf{x}_{\#1}(z_0) = \mathbf{x}_{\#2}(z_0) = \mathbf{x}_0 \\ \mathbf{y}_{\#1}(z_0) = \mathbf{y}_{\#2}(z_0) = \mathbf{y}_0 \end{cases} \tag{14}$$

where z_0 denotes the longitudinal coordinate at the joint point, and $\mathbf{x}_0$, $\mathbf{y}_0$ are vectors collecting the x- and y-reference coordinates of each wire.

2) CONNECTING AN ARBITRARILY SHAPED BUNDLE WITH A BUNDLE APPROXIMATELY PARALLEL TO GROUND

To connect an arbitrarily-oriented bundle (hereinafter, bundle #1) with a bundle approximately parallel to ground (bundle #2) at one end, the first step is to determine the cross-section of bundle #1, which is normal to the ground plane (i.e., perpendicular to z-axis) at the interface section. As a matter of fact, according to the notation in Sec. II-B and Fig. 7, at a given longitudinal (z-axis) position, the independent variable u generally takes different values for every wire inside the bundle. To determine these values, a specific cut-plane transverse to ground and intersecting all wires is preliminarily selected $z = z_{\text{end1}}$. The longitudinal coordinate constraint for each wire i is then formulated as

$$z_i(u_{i,\text{end1}}) = z_{\text{end1}} \tag{15}$$

The obtained nonlinear equations are numerically solved for $u_{i,\text{end1}}$ for $i \in [1, N]$ in the pertinent parameter range. Eventually, wire coordinates at $z = z_{\text{end1}}$ are evaluated as $\mathbf{Q}_i(u_{i,\text{end1}})$, $i \in [1, N]$.

To move bundle #2 in a nearby position, suitable offsets in the x- and y-direction are applied to the original geometry. To achieve smooth connection of the wires belonging to the two bundles, a short bundle segment is generated, by exploiting the polynomial representation in Sec. II-A (with minimum polynomial order equal to three, i.e., spline) in combination with proper terminal constraints.

Wire connection with the minimum displacement is required to avoid additional twisting and complexity. With reference to Fig. 7, this is achieved by connecting wires with identical index in the two bundles. For accurate wire numbering, an *ad-hoc* mapping algorithm is used to handle the scaling and rotation associated with bundle #1. The obtained bundle segment is eventually checked to assure the *non-overlapping* constraint is satisfied. In case of overlapping, an iterative process is performed to slightly modify wire trajectories.

The interconnection of two arbitrarily-oriented wire bundles is similarly performed, by introducing an additional bundle segment satisfying suitable constraints at the terminals.

III. PREDICTION OF EMC CHARACTERISTICS

A. FULL-WAVE SOLUTION

For EMC prediction, the generated bundle geometry can be readily imported into commercial EM software tools (e.g., CST Microwave Studio or Altair FEKO) as 3D analytic curves. For instance, in FEKO, the generation of a bundle sample can be achieved by exploiting the built-in functionality of the *scripting interface*. The obtained 3D model of the harness geometry is then completed by suitable representation of the terminal networks (for a bundle composed of TWPs, an example of implementation of terminal networks is shown in [1]) and solved by adopting a proper meshing scheme.

B. MULTICONDUCTOR TRANSMISSION LINE (MTL) SOLUTION

1) PER-UNIT-LENGTH PARAMETER EVALUATION

To predict voltages/currents at the terminals of the generated N-wire bundle by TL theory, the cable is modelled as a $(N+1)$-conductor non-uniform TL (NUTL). Also, it is preliminarily sampled into N_S sub-sections with nearly-constant cross-sections, which are modeled as uniform TLs and then cascaded, [15]. The number N_S of sub-sections is usually selected as a trade-off between accuracy and computational efficiency [12]. For instance, as far as statistical analysis is the target (which requires the use of *cycles* to generate different bundle samples), the number of subsections can be chosen once and for all with the objective to assure a predefined solution accuracy as follows. First, a specific realization is considered, and a significantly large number (e.g., $N_S = 10\,000$ for a 1-m long bundle) of subsections is initially chosen. Voltages/currents predicted by exploiting such a number of sub-sections are then taken as reference for subsequent evaluations, where the number of subsections is progressively reduced until the maximum variations w.r.t. to the reference currents/voltages are beyond a certain threshold (e.g., in this work, a 1% threshold is considered).

Another aspect requiring special attention is the evaluation of the $N \times N$ impedance and admittance matrices of pertinent p.u.l. parameters, i.e.,

$$\begin{aligned} \hat{\mathbf{Z}}(z) &= \mathbf{R}(z) + j\omega\mathbf{L}(z) \\ \hat{\mathbf{Y}}(z) &= \mathbf{G}(z) + j\omega\mathbf{C}(z) \end{aligned} \tag{16}$$

whose entries are both frequency and place dependent. Hence, accurate yet computational-efficient evaluation is required, which is here achieved by the MoM-based

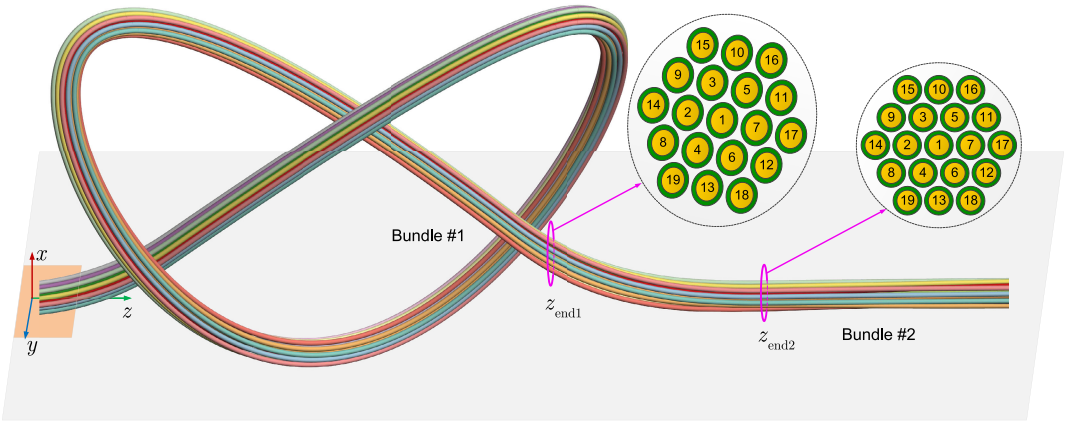

FIGURE 7. Connecting a 19-wire arbitrarily shaped bundle (a trefoil knot shaped bundle, #1) with a random bundle approximately parallel to ground (bundle #2).

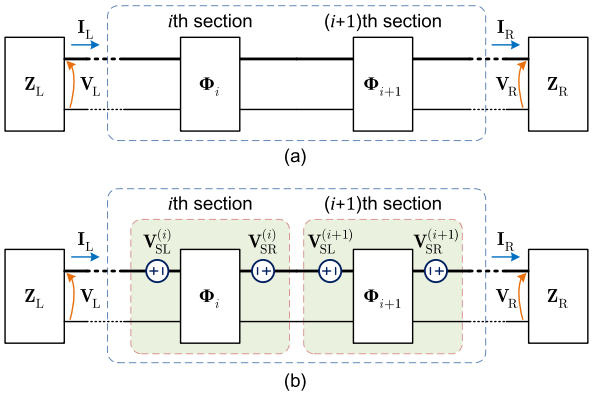

FIGURE 8. MTL-based schematic representation of the cable bundle used for (a) crosstalk, and (b) FWC prediction.

technique developed in [16] for circular-shaped wires. In the specific case of arbitrarily-oriented wire bundles, effective p.u.l. parameter estimation passes through the projection of the actual cross-sections on vertical cut-planes, which requires to calculate the actual line coordinate u associated with each wire in the bundle for the specific cross-section under analysis.

2) CROSSTALK AND FIELD-TO-WIRE COUPLING (FWC)-INDUCED VOLTAGES/CURRENTS

To predict voltages and currents induced by crosstalk at the bundle terminals, the chain-parameter matrices associated to every uniform sub-sections are cascaded, and suitable port constraints are enforced at the bundle ends. A schematic representation is shown in Fig. 8(a), where the terminal networks are modeled in terms of Thevenin equivalent circuits (i.e., by $N \times 1$ voltage-source vectors $\mathbf{V}_{\mathrm{L}}^{\mathrm{S}}$ and $\mathbf{V}_{\mathrm{R}}^{\mathrm{S}}$ for the active part, and $N \times N$ impedance matrices $\mathbf{Z}_{\mathrm{L}}$ and $\mathbf{Z}_{\mathrm{R}}$ for the passive part).

To predict voltages and currents induced by FWC, distributed voltage sources, representative for the effects of the external EM field, and connected at both sides of each sub-section are introduced, as shown in Fig. 8(b). Evaluation of distributed sources can be achieved by resorting to

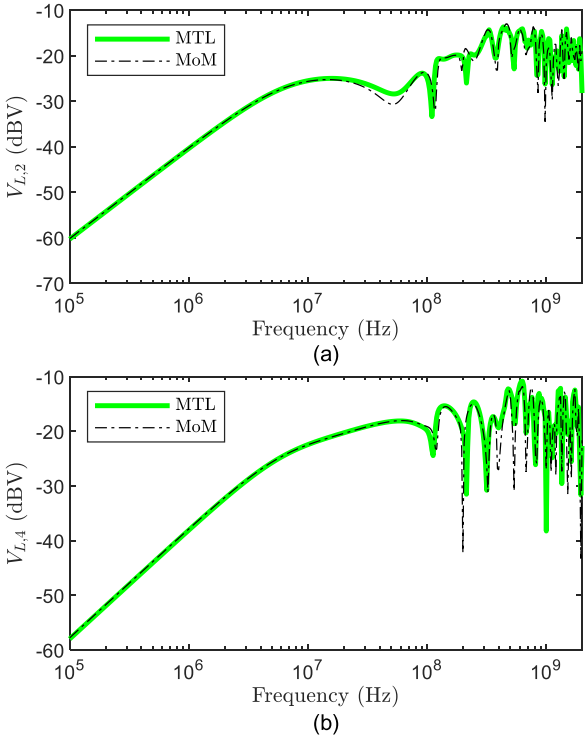

FIGURE 9. Crosstalk prediction: voltages induced at left-end of a seven-wire random bundle with a trefoil knot in the middle: MTL vs MoM simulation for wire (a) #2 and (b) #4.

analytical or numerical methods, e.g., [1], [13], [17], [18]. Particularly, for arbitrarily-oriented (3D) wire trajectories of wires, accurate evaluation of field contributions requires to carefully account for the actual geometrical alignment of the field to the wires in the bundle. Besides, to increase prediction accuracy, the actual, instead of the longitudinal, wire length is evaluated by analytical/numerical integration of trajectory analytical expressions, and accounted for in the calculation of the chain-parameter matrices.

IV. APPLICATION EXAMPLES

As a first example, the proposed method is exploited to generate a random bundle composed of seven wires, and exhibiting

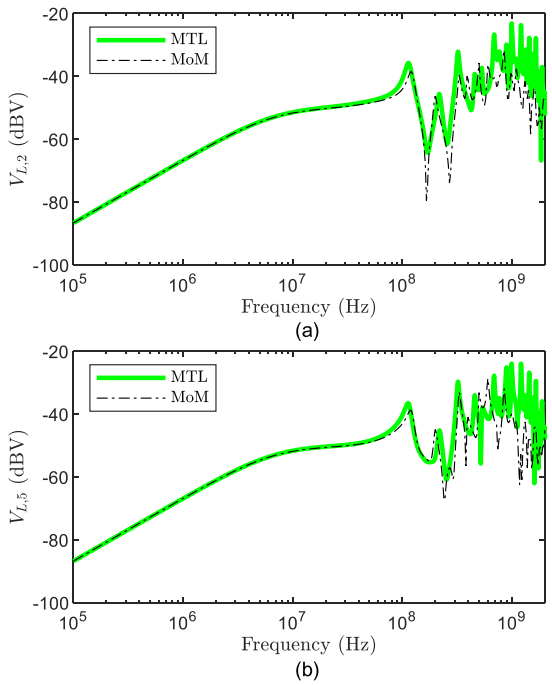

FIGURE 10. FWC prediction: voltages induced at left-end of a seven-wire random bundle with a trefoil knot in the middle: MTL vs MoM simulation for wire (a) #2 and (b) #5.

a trefoil knot along its length. The bundle longitudinal length is 1 m, with average total wire length of 1.35 m. The two bundle sections by the sides of the knot have average height with respect to ground of 2.3 cm. The knot exhibits a maximum and minimum height with respect to ground of 9.1 cm (peaks) and 0.9 cm (valley), respectively. Two short (5 cm) bundle sections generated by 3-rd order polynomial representation are used to interconnect the knot with the lateral bundle sections. All wires in the bundle have inner radius 0.25 mm and outer radius 0.5 mm (for simplicity, air insulation will be considered in the following examples). At both terminations, each wire in the bundle is connected to ground by a load impedance $Z = 150\ \Omega$. Eventually, for the crosstalk prediction, a voltage source with 1 V-amplitude is connected at the left end of wire #1; for the FWC study, a plane-wave EM field (the reference system for the definition of the elevation and incident angles characterizing the plane-wave field can be found in [1]) characterized by E-field strength $E_0 = 1$ V/m and incidence angles $\vartheta = 50°$, $\psi = 20°$, $\eta = 60°$ is assumed to illuminate the wiring structure.

To predict the voltages induced at the harness terminations by the external field, the whole structure is modelled as a nonuniform MTL, and the bundle geometry is discretely sampled in order to evaluate pertinent p.u.l. parameters. Specifically, lateral bundle sections are sub-divided into 100 sub-sections, whereas 50 sub-sections are used to evenly sample the knot along its longitudinal length. Pertinent p.u.l. parameters are numerically evaluated for the corresponding cross-sections. To this end, the cross-sections associated with the knot were preliminarily projected onto vertical cut-planes perpendicular to the ground plane, and the actual coordinates u associated with each wire in the bundle were evaluated.

Predictions of the voltages induced at the bundle ends are then compared versus those obtained by the numerical solver. Examples of comparison are shown in Figs. 9 and 10, where voltages of different wires induced at the left termination are plotted. On the whole, a satisfactory agreement is achieved. More specifically, the comparison proves that MTL solution can provide very accurate prediction of the induced voltages up to hundreds of megahertz, with discrepancies (anyway limited to a few of decibels) in the gigahertz region, where the assumptions of TL theory are no longer satisfied. This is mainly due to the presence of the knot, whose geometrical characteristics were selected on purpose to exacerbate line non-uniformity with respect to ground.

As a second example, the previously mentioned wire bundle structure is replaced by a TWP bundle. The bundle geometry can be readily obtained starting from the same reference wire trajectory considered before, yet modelling the two wires in each twisted pair as place-dependent variations of the previous wire trajectories [according to (5) and (11)]. To this end, the radius of each wire in the TWP is reduced to 0.15 mm, and the separation between the two wires in the pair is made identical to the outer radius (i.e., 0.5 mm) of each wire in the original bundle. Moreover, a pitch rate of 25 per unit meter is set, and the initial angle of each TWP at the left end is randomly generated between 0 and 2π. The 3-D view of the generated bundle structure is shown in Fig. 11. For crosstalk prediction, a voltage source with 1 V-amplitude is connected to the left-end load of the first wire in TWP #1. For FWC prediction, the same plane-wave field as in the previous example is considered. Also, the same subdivision into sub-sections (i.e., 100 sub-sections for lateral line sections, and 50 sub-sections for the knot) is adopted, with all wires terminated at both ends in 150 Ω load impedances.

Predictions of the common-mode (CM) voltages induced at left terminals of two TWPs in the bundle obtained by MTL and MoM solution are compared in Figs. 12 and 13. In spite of the strong non-uniformity affecting the wiring structure, the comparison confirms the accuracy of MTL-based prediction in a wide frequency range along with a significant

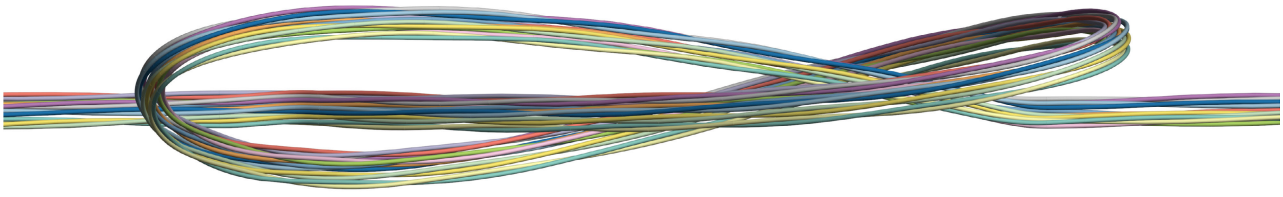

FIGURE 11. Illustration of the bundle with 7 TWPs used for Crosstalk and FWC prediction.

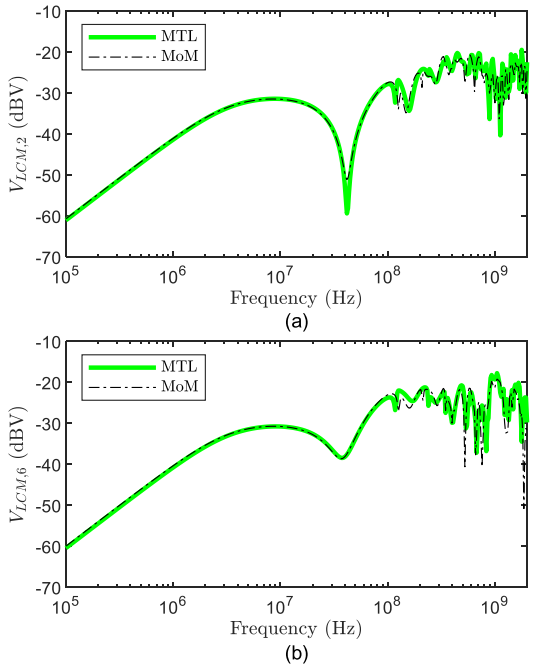

FIGURE 12. Crosstalk prediction: CM voltages induced at left-end of a random bundle composed of 7 TWPs with a trefoil knot in the middle: MTL vs MoM simulation for (a) TWP #2 and (b) TWP #6.

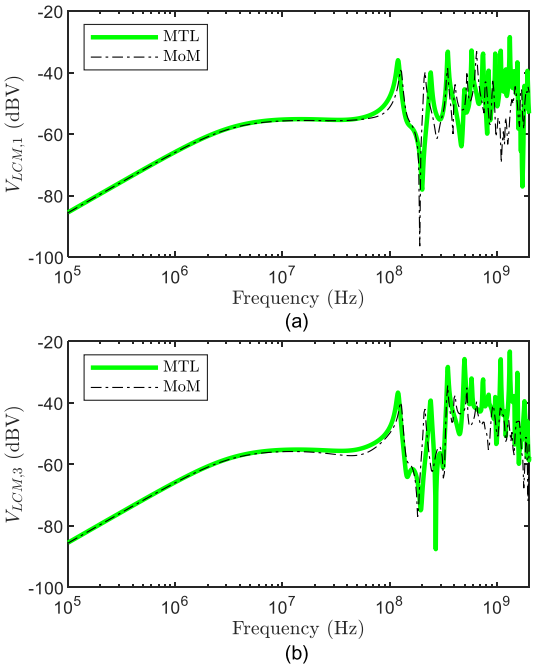

FIGURE 13. FWC prediction: CM voltages induced at left-end of a random bundle composed of 7 TWPs with a trefoil knot in the middle: MTL vs MoM simulation for (a) TWP #1 and (b) TWP #3.

decrease in terms of computational burden. Namely, for the considered example (i.e., FWC prediction in the interval from 100 kHz up to 2 GH with 100 points/decade frequency sampling) and a standard desktop PC with an Intel(R) Core(TM) i5-7400 CPU running at 3.0 GHz and 16 GB of RAM, the simulation exploiting MTL-based solution required 24.2 s, while the MoM-based solver required 11 hours.

V. CONCLUSION

In this work, a general framework has been introduced to achieve accurate representation of the geometry of complex wiring harnesses, such as hand-assembled wire/TWP bundles exhibiting random displacement of wires along the cable length. Both cables nearly parallel to ground and those characterized by arbitrarily-oriented cable-axis have been modelled, by resorting to analytical curves to accurately represent wire trajectories. The proposed procedure assures continuity of wire trajectories and compactness of the bundle along its axis. Additionally, wire overlapping along the cable length is prevented through an iterative *ad-hoc* algorithm, which introduces slight perturbations of wire trajectories whenever overlapping is detected. The original formulation of the generation procedure has been readily extended also to model bundles of TWPs, as well as complex geometries obtained by interconnecting different bundle segments, thus providing a comprehensive tool to represent realistic wiring harnesses. Though not considered in this paper for brevity, the proposed methodology can also be promising when considering the more comprehensive scenario of bundles-of-bundles, specifically bundles made of wire-pairs, or twisted wire-pairs, Ethernet cables, or single-pair Ethernet running near other wiring structures such as, for example, power cables in electric vehicles.

For predicting EMC performance, i.e., the immunity of terminal units to crosstalk among wires as well to external EM fields, it has been shown that the obtained geometries can be easily imported into commercial 3D software tools, and solved by resorting to full-wave numerical methods. Additionally, the examples proposed in this article proved that, in spite of their complexity, the generated bundle geometries can be easily combined with TL-based techniques, and used to achieve approximate yet more computational efficient prediction of the voltages and currents induced at the bundle terminations by EM interference.

REFERENCES

[1] G. Spadacini, F. Grassi, and S. A. Pignari, "Field-to-wire coupling model for the common mode in random bundles of twisted-wire pairs," *IEEE Trans. Electromagn. Compat.*, vol. 57, no. 5, pp. 1246–1254, Oct. 2015.

[2] G. Li, G. Hess, R. Hoeckele, S. Davidson, P. Jalbert, V. V. Khilkevich, T. P. Van Doren, D. Pommerenke, and D. G. Beetner, "Measurement-based modeling and worst-case estimation of crosstalk inside an aircraft cable connector," *IEEE Trans. Electromagn. Compat.*, vol. 57, no. 4, pp. 827–835, Aug. 2015.

[3] C. Yang, W. Yan, Y. Zhao, Y. Chen, C. Zhu, and Z. Zhu, "Analysis on RLCG parameter matrix extraction for multi-core twisted cable based on back propagation neural network algorithm," *IEEE Access*, vol. 7, pp. 126315–126322, 2019.

[4] C. Huang, Y. Zhao, W. Yan, Q. Liu, and J. Zhou, "A new method for predicting crosstalk of random cable bundle based on BAS-BP neural network algorithm," *IEEE Access*, vol. 8, pp. 20224–20232, 2020.

[5] Y. Wang, Y. S. Cao, D. Liu, R. W. Kautz, N. Altunyurt, and J. Fan, "Evaluating the crosstalk current and the total radiated power of a bent cable harness using the generalized MTL method," *IEEE Trans. Electromagn. Compat.*, vol. 62, no. 4, pp. 1256–1265, Aug. 2020.

[6] S. Salio, F. Canavero, J. Lefebvre, and W. Tabbara, "Statistical description of signal propagation on random bundles of wires," in *Proc. 13th Int. Zurich Symp. Electromagn. Compat.*, Zurich, Switzerland, 1999, p. 6.

[7] S. Salio, F. Canavero, D. Lecointe, and W. Tabbara, "Crosstalk prediction on wire bundles by kriging approach," in *Proc. IEEE Int. Symp. Electromagn. Compat. Symp. Rec.*, vol. 1, Aug. 2000, pp. 197–202.
[8] S. Sun, G. Liu, J. L. Drewniak, and D. J. Pommerenke, "Hand-assembled cable bundle modeling for crosstalk and common-mode radiation prediction," *IEEE Trans. Electromagn. Compat.*, vol. 49, no. 3, pp. 708–718, Aug. 2007.
[9] C. Jullien, P. Besnier, M. Dunand, and I. Junqua, "Towards the generation of industrial bundles through a random process under realistic constraints," in *Proc. 9th Int. Symp. EMC Joint 20th Int. Wroclaw Symp. (EMC)*, 2010, p. 97.
[10] C. Jullien, P. Besnier, M. Dunand, and I. Junqua, "Crosstalk analysis in complex aeronautical bundle," in *Proc. Int. Symp. Electromagn. Compat.*, 2013, pp. 253–258.
[11] O. Gassab, S. Bouguerra, L. Zhou, Z.-G. Zhao, and W.-Y. Yin, "Stochastic analysis of multitwisted cables with random parameters excited by random plane-wave fields," *IEEE Trans. Electromagn. Compat.*, vol. 62, no. 5, pp. 2084–2095, Oct. 2020.
[12] X. Liu, F. Grassi, G. Spadacini, and S. A. Pignari, "Physically based modeling of hand-assembled wire bundles for accurate EMC prediction," *IEEE Trans. Electromagn. Compat.*, vol. 62, no. 3, pp. 914–922, Jun. 2020.
[13] G. Spadacini, "Numerical assessment of radiated susceptibility of twisted-wire pairs with random nonuniform twisting," *IEEE Trans. Electromagn. Compat.*, vol. 55, no. 5, pp. 956–964, Oct. 2013.
[14] W. Wang, B. Jüttler, D. Zheng, and Y. Liu, "Computation of rotation minimizing frames," *ACM Trans. Graph.*, vol. 27, no. 1, pp. 1–18, Mar. 2008.
[15] C. R. Paul, *Analysis of Multiconductor Transmission Lines*. Hoboken, NJ, USA: Wiley, 2008.
[16] J. Clements, C. Paul, and A. Adams, "Computation of the capacitance matrix for systems of dielectric-coated cylindrical conductors," *IEEE Trans. Electromagn. Compat.*, vol. EMC-17, no. 4, pp. 238–248, Nov. 1975.
[17] A. Agrawal, H. Price, and S. Gurbaxani, "Transient response of multiconductor transmission lines excited by a nonuniform electromagnetic field," *IEEE Trans. Electromagn. Compat.*, vol. EMC-22, no. 2, pp. 119–129, May 1980.
[18] X. Liu, F. Grassi, G. Spadacini, and S. A. Pignari, "Approximate transmission-line model for field-to-wire coupling in arbitrarily routed wiring structures above ground," *IEEE Trans. Electromagn. Compat.*, early access, Sep. 9, 2021, doi: 10.1109/TEMC.2021.3103131.

XIAOKANG LIU (Member, IEEE) received the double M.Sc. degrees in electrical engineering from Xi'an Jiaotong University, Xi'an, China, and the Politecnico di Milano, Milan, Italy, in 2016, and the Ph.D. degree *(summa cum laude)* in electrical engineering from the Politecnico di Milano, in 2021.

He is currently a Postdoctoral Research Fellow with the Department of Electronics, Information, and Bioengineering, Politecnico di Milano. His research interests include electromagnetic compatibility, power electronics, and signal integrity.

Dr. Liu was a recipient of the International Union of Radio Science Young Scientist Award, in 2021, and the 2021 Richard B. Schulz Best EMC Transactions Paper Award.

FLAVIA GRASSI (Senior Member, IEEE) received the Laurea (M.Sc.) and Ph.D. degrees in electrical engineering from the Politecnico di Milano, Milan, Italy, in 2002 and 2006, respectively.

She is currently a Full Professor with the Department of Electronics, Information and Bioengineering, Politecnico di Milano. From 2008 to 2009, she was with European Space Agency (ESA), ESA/ESTEC, The Netherlands, as a Research Fellow. Her research interests include distributed-parameter circuit modeling, statistical techniques, characterization of measurement setups for EMC testing (aerospace and automotive sectors), and application of the powerline communications technology in ac and dc lines.

Dr. Grassi received the International Union of Radio Science (URSI) Young Scientist Award, in 2008, and the IEEE Young Scientist Award at the 2016 Asia-Pacific International Symposium on EMC (APEMC), the IEEE EMC Society 2016 and 2021 Transactions Prize Paper Award, and the Best Symposium Paper Award at the 2015 and 2018 APEMC.

GIORDANO SPADACINI (Senior Member, IEEE) received the Laurea (M.Sc.) and Ph.D. degrees in electrical engineering from the Politecnico di Milano, Italy, in 2001 and 2005, respectively.

He is currently an Associate Professor with the Department of Electronics, Information, and Bioengineering, Politecnico di Milano. His research interests include statistical models for the characterization of interference effects, distributed parameter circuit modeling, experimental procedures and setups for EMC testing, and EMC in aerospace, automotive, and railway systems. He was a recipient of the 2005 EMC Transactions Prize Paper Award, the 2016 and 2021 Richard B. Schulz Best EMC Transactions Paper Award, two Best Symposium Paper Awards from the 2015 Asia-Pacific International Symposium on EMC (APEMC), and the 2018 Joint IEEE EMC & APEMC Symposium.

SERGIO AMEDEO PIGNARI (Fellow, IEEE) received the Laurea (M.S.) and Ph.D. degrees in electronic engineering from Politecnico di Torino, Turin, Italy, in 1988 and 1993, respectively.

From 1991 to 1998, he was an Assistant Professor with the Department of Electronics, Politecnico di Torino. In 1998, he joined the Politecnico di Milano, Milan, Italy, where he is currently a Full Professor of circuit theory and electromagnetic compatibility (EMC) with the Department of Electronics, Information, and Bioengineering. He served as the Chair for the B.Sc. and M.Sc. Study Programmes in electrical engineering, term (2015–2020). He is the author or coauthor of more than 220 papers published in international journals and conference proceedings. His research interests are in the field of EMC and include field-to-wire coupling and crosstalk, conducted immunity and emissions in multi-wire structures, statistical techniques for EMC prediction, and experimental procedures and setups for EMC testing. His research activity is mainly related to aerospace, automotive, energy, and railway industry sectors.

Dr. Pignari was a co-recipient of the 2005, 2016, and 2021 IEEE EMC Society Transactions Prize Paper Award, and the 2011 IEEE EMC Society Technical Achievement Award. He is currently serving as an Associate Editor for the IEEE TRANSACTIONS ON ELECTROMAGNETIC COMPATIBILITY. From 2010 to 2015, he served as the IEEE EMC Society Chapter Coordinator. From 2007 to 2009, he was the Chair of the IEEE Italy Section EMC Society Chapter. He served as the Italian URSI Officer for Commission E (Electromagnetic Noise and Interference), term (2015–2018). He has been the Technical Program Chair of the ESA Workshop on Aerospace EMC, since 2009, and a member of the Technical Program Committee of the Asia Pacific EMC Week, since 2010.